NEOPLASIA
www.neoplasia.com

Volume 10 Number 10 October 2008 pp. 1146–1153 **1146**

Progression of Epididymal Maldevelopment Into Hamartoma-like Neoplasia in VHL Disease[1]

Gautam U. Mehta*, Sharon B. Shively*,†, Heng Duong*, Maxine G.B. Tran‡, Travis J. Moncrief*, Jonathan H. Smith*, Jie Li*, Nancy A. Edwards*, Russell R. Lonser*, Zhengping Zhuang*, Marsha J. Merrill*, Mark Raffeld§, Patrick H. Maxwell¶, Edward H. Oldfield* and Alexander O. Vortmeyer*,[2]

*Surgical Neurology Branch, National Institute of Neurological Disorders and Stroke, National Institutes of Health, Bethesda, MD, USA; †Molecular and Cellular Oncology, Institute for Biomedical Sciences, George Washington University, Washington, DC, USA; ‡CRUK Uro-Oncology Research Group, Cancer Research UK, Li Ka Shing Centre, Cambridge Research Institute, Cambridge, United Kingdom; §Laboratory of Pathology, National Cancer Institute, Bethesda, MD, USA; ¶Renal Section, Imperial College of Science Technology and Medicine, Hammersmith Hospital, London, UK

Abstract

Inactivation of the von Hippel–Lindau (*VHL*) gene and activation of the hypoxia-inducible factor (HIF) in susceptible cells precedes formation of tumorlets and frank tumor in the epididymis of male VHL patients. We performed detailed histologic and molecular pathologic analysis of tumor-free epididymal tissues from VHL patients to obtain further insight into early epididymal tumorigenesis. Four epididymides from two VHL patients were serially sectioned to allow for three-dimensional visualization of morphologic changes. Areas of interest were genetically analyzed by tissue microdissection, immunohistochemistry for HIF and markers for mesonephric differentiation, and *in situ* hybridization for HIF downstream target vascular endothelial growth factor. Structural analysis of the epididymides revealed marked deviations from the regular anatomic structure resulting from impaired organogenesis. Selected efferent ductules were represented by disorganized mesonephric cells, and the maldeveloped mesonephric material was VHL-deficient by allelic deletion analysis. Furthermore, we observed maldeveloped mesonephric material near cystic structures, which were also VHL-deficient and were apparent derivatives of maldeveloped material. Finally, a subset of VHL-deficient cells was structurally integrated in regular efferent ductules; proliferation of intraductular VHL-deficient cells manifests itself as papillary growth into the ductular lumen. Furthermore, we clarify that that there is a pathogenetic continuum between microscopic tumorlets and formation of tumor. In multiple locations, three-dimensional reconstruction revealed papillary growth to extend deeply into ductular lumina, indicative of progression into early hamartoma-like neoplasia. We conclude epididymal tumorigenesis in VHL disease to occur in two distinct sequential steps: maldevelopment of VHL-deficient mesonephric cells, followed by neoplastic papillary proliferation.

Neoplasia (2008) 10, 1146–1153

Address all correspondence to: Alexander O. Vortmeyer, MD, Surgical Neurology Branch, National Institute of Neurological Disorders and Stroke, National Institutes of Health, 10 Center Drive, Room 5D37, Bethesda, MD 20892. E-mail: alexander.vortmeyer@yale.edu

[1]This work was supported by the Intramural Research Program of the National Institute of Neurological Disorders and Stroke, National Institutes of Health; by Cancer Research, UK; the Medical Research Council; and by the Charitable foundation of Guy's and St Thomas' Hospitals, London. Sharon B. Shively is a doctoral student in the Molecular and Cellular Oncology Program of the Institute for Biomedical Sciences at George Washington University. This work is from a dissertation to be presented at George Washington University in partial fulfillment of the requirements for the Ph.D. degree.

[2]New address: Department of Pathology, Yale University School of Medicine, 416A Lauder Hall, 310 Cedar Street, New Haven, CT 06520.

Received 11 April 2008; Revised 16 July 2008; Accepted 17 July 2008

DOI 10.1593/neo.08476

Introduction

von Hippel–Lindau (VHL) disease is a tumor-suppressor gene syndrome that causes pathologic changes in central and peripheral nervous systems and retina, kidney, pancreas, adrenal glands, vestibular aqueduct, and the epididymis. The epididymis frequently develops a benign tumor, epididymal cystadenoma [1,2]. Consistent with Knudson's "two-hit hypothesis", patients with VHL disease carry a germ line mutation of the *VHL* gene [3]. Inactivation of the other, wild type copy of the *VHL* gene in susceptible cells within the epididymis has been associated with cystadenoma development [4]. With this study, we further characterize the cells in which the "second hit," responsible for knockout of VHL protein function, occurs.

In recent studies on nervous system tissues of VHL patients, we suggest that VHL tumorigenesis is preceded by developmental changes and propose that the structural and topographic complexity of the pathologic changes can only be explained by VHL inactivation of selected cells during CNS development [5,6]. Because of the relatively large size of the human central and peripheral nervous system, however, detailed analysis requires extensive sampling of tissues [5], and various sites of CNS tumorigenesis remain poorly understood. In contrast, tumorigenesis in human epididymis seems to be restricted to the efferent ductule compartment [4], an anatomic structure of approximately 1 cm^3 in size. In the epididymis, therefore, the effects of VHL deficiency on the entire organ can be analyzed in unprecedented detail.

von Hippel–Lindau disease–associated early pathologic changes within the nervous system and outside the nervous system show fundamental differences. Within the nervous system, the earliest detectable changes have been characterized as vascularized "mesenchymal tumorlets" [5,6]; in contrast, early changes in the epididymis are characterized as cystic or papillary "epithelial tumorlets" [4]. The "mesenchymal tumorlets" in the CNS have been shown to have the potential of progressing into VHL-deficient mesenchyme and tumor [5]. Whereas epithelial tumorlets in the epididymis have been shown to be VHL-deficient [4], it has never been clarified whether microscopic structural changes are pathogenetically distinct from frank tumors or whether they represent a pathogenetic continuum. With this study, we attempted to identify and characterize different types of mesonephric maldevelopment in VHL epididymis to provide direct evidence that tissue maldevelopment is pathogenetically linked to tumorigenesis.

Materials and Methods

Tissue

Four grossly intact epididymides were procured at autopsy of two adult male VHL patients. One patient had died at 40 years from acute renal failure after bilateral nephrectomy for renal cell carcinoma and pheochromocytoma. He had developed cerebellar hemangioblastomas, bilateral endolymphatic sac tumors, and pancreatic microcystic adenoma. The other patient had died at 43 years from intracerebral hemorrhage, with a clinical history of cerebellar and spinal cord hemangioblastomas and bilateral renal cell carcinoma. Most of each epididymis was procured for this study, whereas smaller parts were retained at the Laboratory of Pathology, National cancer Institute, for diagnostic purposes. Research material was fixed in formalin and processed into paraffin blocks. Each paraffin block containing efferent ductules was serially sectioned. Of the serial sections, at least every 10th section was stained with hematoxylin and eosin (H&E) for morphologic evaluation. This approach allowed reconstruction of anatomic changes in three dimensions. In addition, adjacent sections were available from each microscopic structure of interest for additional immunohistochemical or molecular pathologic investigations.

Immunohistochemistry

Immunohistochemistry on paraffin sections was performed using anti-CD31 (DAKO, Carpinteria, CA; 1:20 dilution; predigestion with protease I) and cytokeratin cocktails HMWK (DAKO; 1:100 dilution; heat-induced epitope retrieval), AE1/AE3 (DAKO; 1:80 dilution; predigestion with protease I), and MAK6 (Zymed, South San Francisco, CA; 1:2 dilution; predigestion with protease I). Immunohistochemistry was performed on a Ventana ES using an I-view detection kit (Ventana, Tucson, AZ).

A modified protocol was used for the detection of hypoxia-inducible factors HIF1 and HIF2. For antigen retrieval, sections were immersed in preheated Dako target retrieval solution in a pressure cooker for 90 seconds. Primary antibodies were mouse monoclonal antihuman HIF1α H1α67 (Neomarkers, Fremont, CA) 1/1000 and rabbit polyclonal antimouse HIF2α PM8 antiserum [7], 1/10,000. Primary antibody was omitted for negative controls. Antigen/antibody complexes were revealed by means of the Catalyzed Signal Amplification system (DAKO; HIF) or Envision system (DAKO; CAIX) according to the manufacturer's instructions. Sections were counterstained with hematoxylin for 15 seconds, dehydrated in graded ethanol washes, and mounted in *p*-xylene-bis-pyridinium bromide permount (Lamb, Eastbourne, UK).

The following protocol was used for the detection of AE1/3, HMWK (Dakocytomation, Carpinteria, CA), and MAK6 (Zymed) on paraffin sections. For antigen retrieval, sections were treated with DAKO Target Retrieval Solution (DAKO) and incubated at 95°C for 20 minutes. Sections were cooled at room temperature and washed three times in PBS. After three washes in PBS, sections were incubated in 10% horse serum for 1 hour. The primary antibody was diluted in 2% horse serum, and the sections were incubated in a humidified chamber at 4°C overnight. The sections were then incubated with secondary antibody and avidin-biotin complex for 1 hour each. The reaction product was visualized with diaminobenzidine (DAB). A 30-second counterstaining with Mayer's hematoxylin followed. Sections were dehydrated by graded ethanol washes of 95% and 100% and were washed with xylene before being mounted.

In Situ *Hybridization*

The cDNA encoding human vascular endothelial growth factor (VEGF) was cloned into a SK2 Bluescript plasmid (Stratagene, La Jolla, CA) using *Hind*III and *Eco*RI as restriction sites [8]. The digoxigenin (DIG) probes were transcribed in sense and antisense directions using T3 and T7 RNA polymerase, respectively. This protocol is based on the Roche manual [9]. In brief, after deparaffinization and rehydration, sections were refixed in 4% paraformaldehyde for 20 minutes, washed with TBS, immersed in 0.2 M hydrochloric acid for 10 minutes, and washed again with TBS. The sections were treated with 0.5% acetic anhydride in 100 mM Tris (pH 8.0) for 10 minutes then washed with TBS. The sections were transferred into a Proteinase K solution and digested for 20 minutes at 37°C. The sections were washed with TBS, and the reaction was stopped by incubation in TBS at 4°C for 5 minutes. After dehydration with ethanol, the sections were rinsed briefly with chloroform and placed in a humid chamber at 55°C for 30 minutes. Digoxigenin-labeled VEGF antisense probes were then applied to the tissues. Both DIG-labeled sense probes and

no primary probes were used as negative controls. The sections were placed on a hot plate at 95°C for 4 minutes and incubated in a humid chamber at 55°C overnight. The sections were washed with 2× SSC at room temperature, with 1× SSC with 50% deionized formamide at 55°C, with 1× SSC at room temperature and finally with TBS. The sections were incubated with blocking reagent containing 10% Fraction V albumin for 15 minutes. The sections were next incubated with alkaline phosphatase–conjugated anti-DIG antibody for 60 minutes, followed by washing with TBS and then application of NBT/BCIP color reagent for visualization at 4°C overnight. The sections were counterstained with BC-50 Red Counterstain (Biomeda, Foster City, CA). The presence and intensity of DIG antibody expression were examined in conjunction with the serial H&E sections.

Microdissection and Deletion Analysis

Tissue sections taken from formalin-fixed, paraffin-embedded tissue blocks were placed on glass slides and used for microdissection and loss of heterozygosity (LOH) analysis. The sections were consecutive to those investigated by H&E staining. Microdissection was performed under direct light microscopic visualization using a 30-gauge needle as previously described [4].

Control samples were obtained from normal epididymis tissue on the same histologic slide. Procured cells were immediately resuspended in 10 to 30 μl of buffer containing Tris/HCl, pH 8.0, 10 mM ethylenediamine tetra-acetic acid, pH 8.0, 1% Tween 20, and 0.1 mg/ml proteinase K and were incubated at 37°C for 3 days. The mixture was boiled for 10 minutes to inactivate proteinase K, and 2 μl of this solution was used for the polymerase chain reaction amplification of DNA.

The samples were analyzed for LOH with the microsatellite markers D3S1038 and D3S1110 (Invitrogen, Carlsbad, CA), flanking the *VHL* gene on chromosome 3p25. Polymerase chain reaction was performed for 38 cycles: denaturing at 95°C for 45 seconds, annealing at 55°C for 45 seconds, and extending at 72°C for 45 seconds. For all primers, the final extension was continued for 10 minutes at 72°C. Each PCR sample contained 2 μl of template DNA as noted above, 10 pmol of each primer, 20 nmol each of dATP, dCTP, DGTP, and DTTP, 15 mM $MgCl_2$, 1.25 U of *Taq* DNA polymerase, 0.2 μl of [^{32}P] dCTP (6000 Ci/mmol), and 1 μl of 10× buffer in a total volume of 10 μl. Labeled amplified DNA was mixed with 6 μl of formamide loading dye (95% formamide, 20 mM EDTA, 0.05% bromophenol blue, 0.05% xylene cyanol) and analyzed on a polyacrylamide gel. The samples were denatured for 10 minutes at 95°C and loaded onto a gel consisting of 6% acrylamide (49:1 acrylamide/bis), 5% glycerol, and 0.6× TBE. Samples were electrophoresed at 60 W at room temperature for 1.5 hours. Gels were transferred to a 3-mm Whatman paper and dried, and autoradiography was performed with Kodak X-OMAT film (Eastman Kodak, Rochester, NY).

Results

The Epididymis in Male VHL Patients Shows Maldeveloped Mesonephric Material

Histologic examination of epididymis tissue revealed marked deviations from regular anatomic structure of the efferent ductules. The efferent ductule compartment of regular epididymis is composed of 15 to 20 convoluted ductules [10], and all epithelial cells are integrated within these ductules. In contrast, VHL epididymis displayed areas of diffusely scattered clear cells, arranged in isolation or small clusters, consistent with maldeveloped mesonephric material (Figure 1, *A* and *B*). Parts of individual ductules were represented by diffusely scattered clear cells, arranged isolated or in small clusters (Figure 1*B*). This evidence of incomplete; developmentally arrested efferent ductule formation is consistent with Arvid Lindau's original hypothesis that disturbances of development in the mesoderm lead to failure in the integration between mesodermal and epithelial components [2,11].

Immunohistochemical analysis of maldeveloped cells with MAK6, AE1/AE3, and HMWK showed an immunophenotype that was similar to that of mature efferent ductules, which is consistent with previous observations that mesonephric material and mature nephrons share immunophenotypic features (Figure 1, *C–E*) [12]. Reticulin stain revealed isolated cells and cell clusters to be separated by mature reticulin fibers (Figure 1*F*), anatomically distinct from the mature ductular system in which whole ductules are surrounded by reticulin fibers. Thus, disorganized cell clusters maintain a mesenchymal architecture having failed to form mature epithelial ductules.

Maldeveloped Mesonephric Material Is VHL-Deficient

Hypoxia-inducible factor immunohistochemistry and VEGF *in situ* hybridization revealed positive signal in maldeveloped mesonephric material (Figures 1, *G* and *H*, and 2). Immunoreactivity with anti-HIF2 seemed stronger compared to anti-HIF1 in maldeveloped mesonephric material (Figures 1, *G* and *H*, and 2). Diffuse mesenchymal cell accumulations were microdissected and subjected to LOH analysis of the *VHL* gene locus using primers D3S1110 and D3S1038 flanking the *VHL* gene locus. We identified LOH in disorganized mesonephric material (Figure 1*I*). Therefore, the disorganized mesonephric material is VHL-deficient, and VHL deficiency seems directly associated with structural maldevelopment.

Maldeveloped Mesonephric Material Is Associated with Cyst Formation

Within or at the border of disorganized maldeveloped mesonephric material, we frequently detected cystic-tubular structures, i.e., closed alignments of epithelial cells around an open central space (Figure 2, *A* and *B*). In contrast to mature ductules, however, cysts lacked the characteristic undulating cytologic architecture [10] and were not ciliated. By immunohistochemistry, the cytokeratin expression profile was similar in maldeveloped mesonephric material, cystic-tubular structures, and mature ductules. Microdissection and deletion analysis of cystic-tubular structures consistently revealed LOH of the *VHL* gene locus (data not shown). Therefore, a subset of VHL-deficient cells is capable of forming primitive cystic-tubular structures.

Hypoxia-inducible factor immunohistochemistry and VEGF *in situ* hybridization revealed positive signal in cystic-tubular structures (Figure 2, *C–F*). Similar to our observations in maldeveloped mesonephric material, immunoreactivity with anti-HIF2 seemed stronger compared to anti-HIF1. Three-dimensional reconstruction revealed some cysts to be parts of large tubular structures extending deep into the tissue block, suggestive of immature and incomplete efferent ductule formation (data not shown). Focally, cystic epithelium revealed papillary proliferation.

VHL-Deficient Intraductular Cells Reveal Papillary Proliferation

Not all VHL-deficient cells constitute VHL-deficient maldeveloped mesonephric material or VHL-deficient cystic-tubular structures.

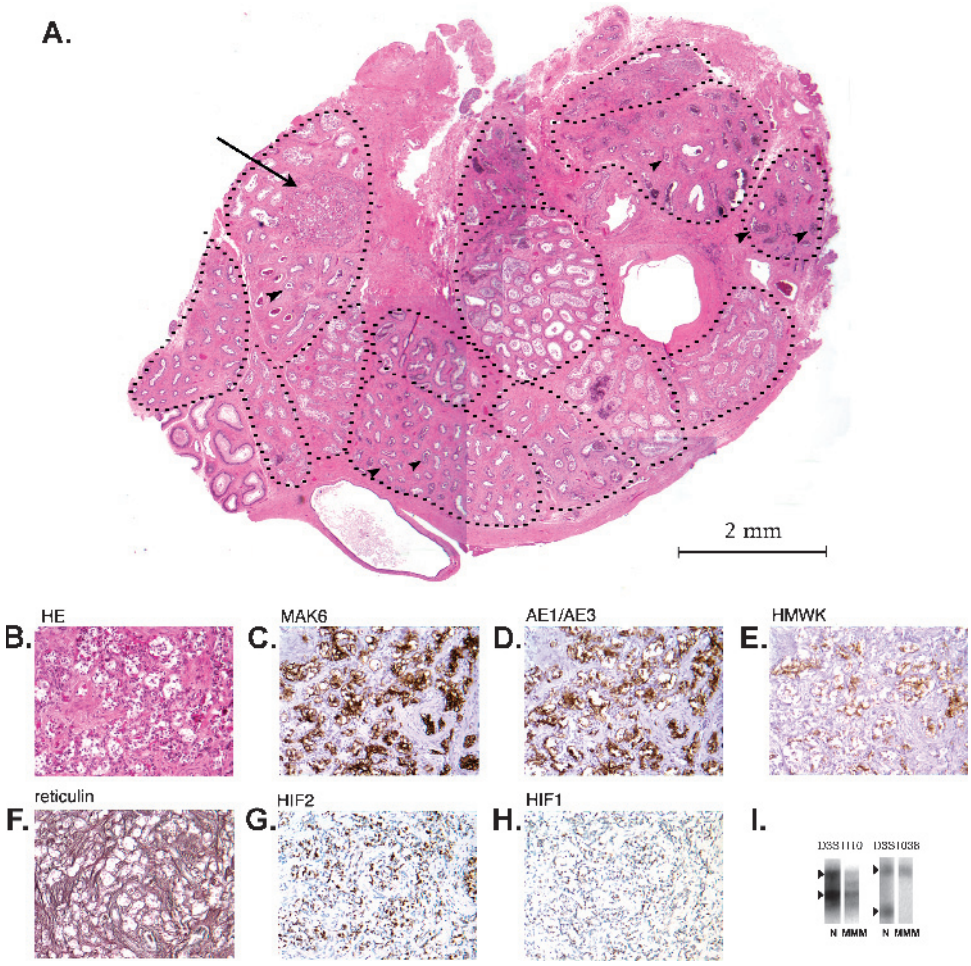

Figure 1. (A) Efferent ductule compartment of tumor-free VHL epididymis, H&E stain. Different efferent ductules are separated by dotted lines. The arrow points to an area of maldeveloped mesonephric material. Arrowheads show multifocal events of intratubular papillary proliferation as previously described [4]. (B) Higher magnification of maldeveloped mesonephric material, characterized by diffusely scattered mesonephric cells, arranged either in isolation or in small clusters. Mesonephric material is immunoreactive with cytokeratin cocktails MAK6 (C), AE1/AE3 (D), and HMWK (E). (F) Reticulin stain reveals sequestration of maldeveloped mesonephric cells and cell clusters. Mesonephric cells reveal activation of HIF2 (G) and HIF1 (H) with stronger signal for HIF2 compared with HIF1. (I) Deletion analysis of maldeveloped mesonephric material (MMM) using markers D3S1110 and D3S1038 reveals LOH of wild type VHL allele compared with normal epididymal tissue (N). Arrowheads point to the position of both VHL alleles for the respective markers.

Instead, a significant number of VHL-deficient cells are integrated within the mature, VHL-competent ductular system (Figures 3 and 4*D*). Proliferation of intratubular VHL-deficient cells was frequently identified as papillary proliferation, i.e., cellular proliferation accompanied by reactive fibrovascular proliferation [4]. Proliferative cells were positive for HIF by immunohistochemistry; notably, the intensity of the HIF1 signal was similar to that of the HIF2 signal (Figure 3) in contrast to diversely intense HIF1 and HIF2 signals observed in maldeveloped material and cysts.

Three-dimensional reconstruction revealed most papillary proliferations to be less than 100 μm in size. In other instances, however, three-dimensional reconstruction allowed us to trace isolated events of papillary formation into larger structures and visualize the anatomy of the structure *in toto* (Figure 5). Larger structures were characterized by deep invaginations of polarized VHL-deficient cells into the ductular system, accompanied by a core of nourishing fibrovascular stroma (Figure 5).

Discussion

von Hippel–Lindau disease elicits an abundance of microscopic foci of cellular proliferation in a selective set of target organs, including the nervous system [5,6], kidney [13,14], epididymis [4], and endolymphatic sac and duct [15]. Morphologically, these cellular proliferations have been identified as mesenchymal tumorlets in the nervous system [5,6] or as epithelial tumorlets in target organs outside the nervous system [4,15]. Our detailed analysis of epididymal tissue from VHL patients provides evidence that microscopic tumorlets are composed of developmentally arrested mesonephric cells. This finding implies that the "second hit"—inactivation of the wild type VHL allele—occurs in mesonephric cells during development of the epididymis.

The multifocality and diversity of microscopic developmental changes (Figure 4) can be explained as a result of coproliferation and codevelopment of VHL-deficient and VHL-competent mesonephric cells. In the VHL epididymis, VHL-deficient mesonephric cells

may persist in isolation, as small VHL-deficient cell clusters or as VHL-deficient cystic-tubular structures (Figures 1, 2, and 4). Some VHL-deficient mesonephric cells, however, are assembled within VHL-competent efferent ductules (Figures 3 and 4). Thus, VHL inactivation in a subset of mesonephric cells during organogenesis results in a different anatomic structure of the efferent ductules in VHL disease.

The generation of tumorlets, in contrast, is the result of the proliferative capacity of VHL-deficient mesonephric cells. Proliferation of cystic or intraductular VHL-deficient cells may generate papillary structures, secondary to recruitment of fibrovascular tissue which supports the expanding surface of proliferating single-layered VHL-deficient cells. Recruitment of fibrovascular tissue is certainly facilitated by the continuous up-regulation of hypoxic stress proteins including HIF, GLUT-1, and VEGF in VHL-deficient mesonephric cells.

Our findings suggest that developing mesonephric cells are primarily targeted in VHL disease and represent cells that have the potential for neoplasia. During human embryogenesis, VHL mRNA is prominently expressed in mesonephric tubules, suggesting a role for the *VHL* gene in early cellular differentiation [16]. How exactly loss of *VHL* gene function is linked to cellular differentiation, maturation, and migration has remained elusive. The VHL protein is part of a multiprotein complex targeting proteins for ubiquitin-mediated degradation [17–19], including HIFα subunit proteins. A possible role for developmental arrest may therefore be played by HIF, which is constitutively activated and stabilized after loss of VHL function [20–22] and consistently present in the smallest tumor precursor structures [4,5]. Similarly, a role for developmental arrest may also be played by HIF target proteins VEGF, GLUT-1, and CAIX [20, 23,24] that have been shown to be expressed in the earliest steps of VHL tumorigenesis [4,5].

There is also emerging evidence that HIF is constitutively active in mesonephric mesenchyme and that VEGF is up-regulated before mesenchymal to epithelial transition [25]; in contrast, expression of these markers is undetectable in mature ductal cells. It could

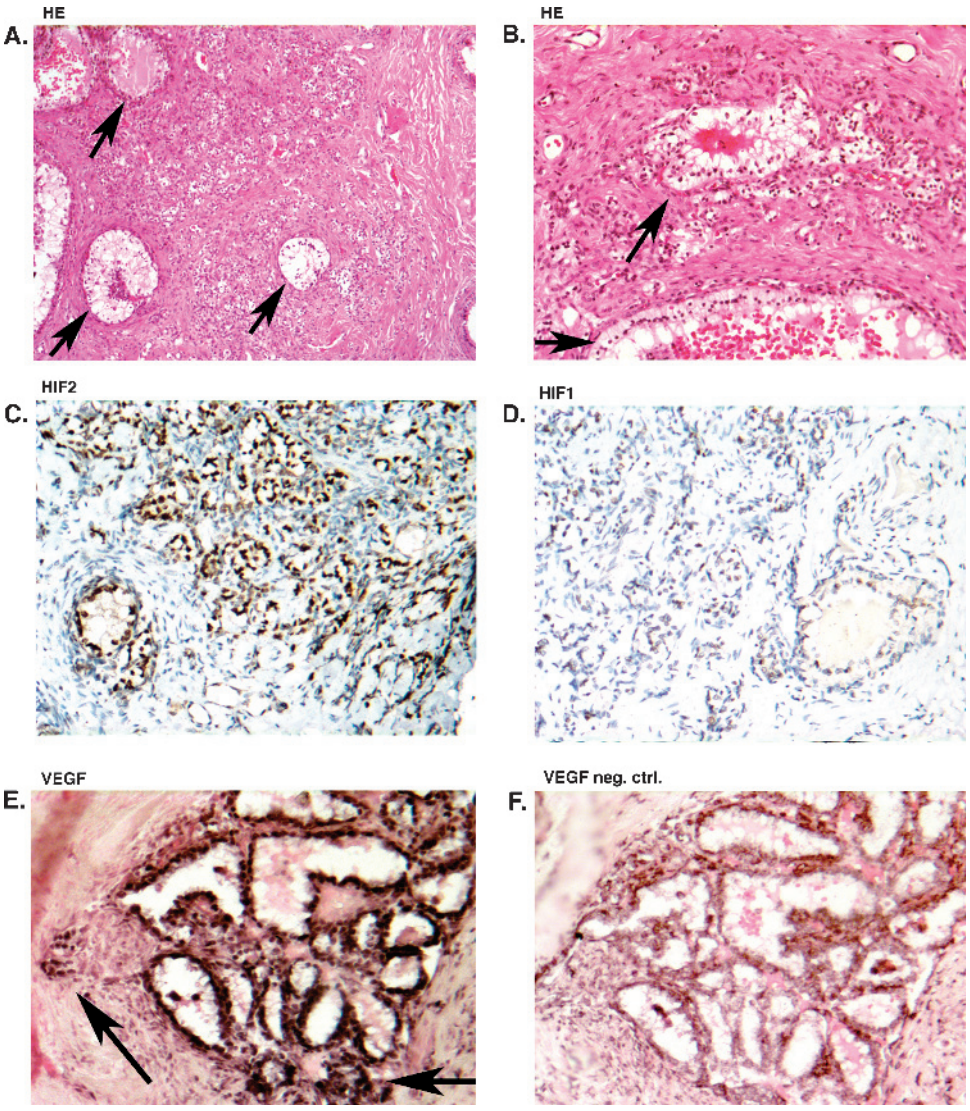

Figure 2. Maldeveloped mesonephric material is associated with cyst formation (A, B; see arrows). Maldeveloped mesonephric material as well as cyst material is VHL-deficient and shows activation of HIF2 (C) and HIF1 (D). (E) *In situ* hybridization with VEGF antisense probe shows expression of VEGF in maldeveloped mesonephric material (arrows) as well as associated cysts; (F) negative control with VEGF sense probe.

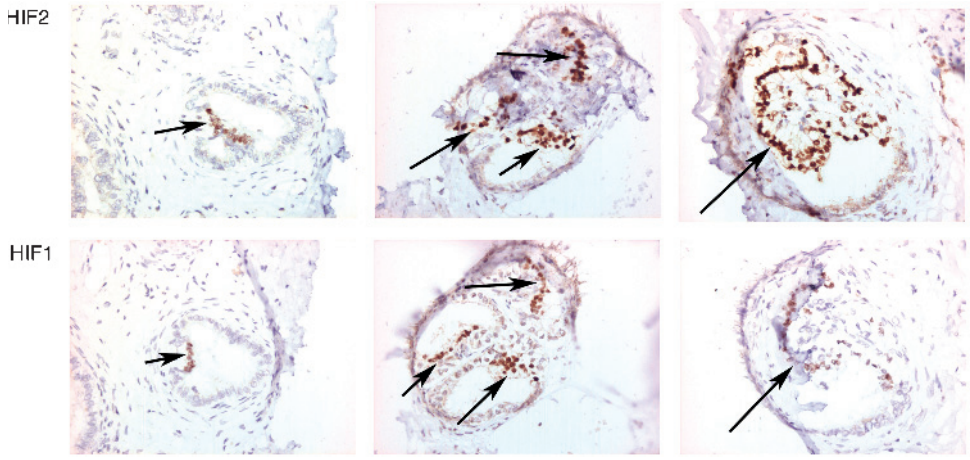

Figure 3. VHL-deficient cells, integrated in mature efferent ductular epithelium, show different stages of papillary growth. Immunohistochemistry for HIF1 and HIF2 was performed on consecutive sections. von Hippel–Lindau–deficient mesonephric cells (identified by immunoreactivity with anti-HIF) accumulate within normal efferent ductules (left, middle) before formation of frank papillary structures (right). The intensity of the HIF1 signal appears similar to that of HIF2 signal.

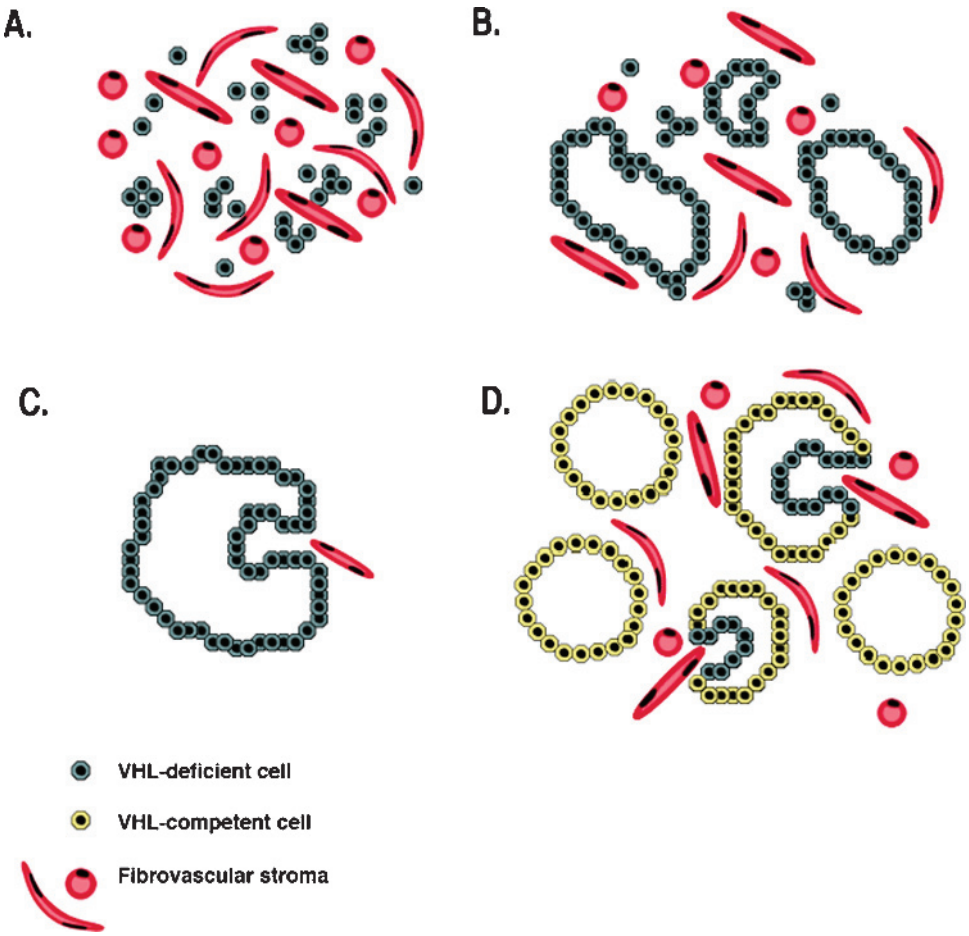

Figure 4. Basic structural-anatomic changes in VHL epididymis. Primary developmental changes are characterized by scattered deposits of VHL-deficient maldeveloped mesonephric cells (A), associated with VHL-deficient tubular structures that appear as cysts in individual sections (B); papillary growth is initiated from tubular/cyst wall epithelium (C) or from VHL-deficient cells that are integrated in regular efferent ductular structures (D).

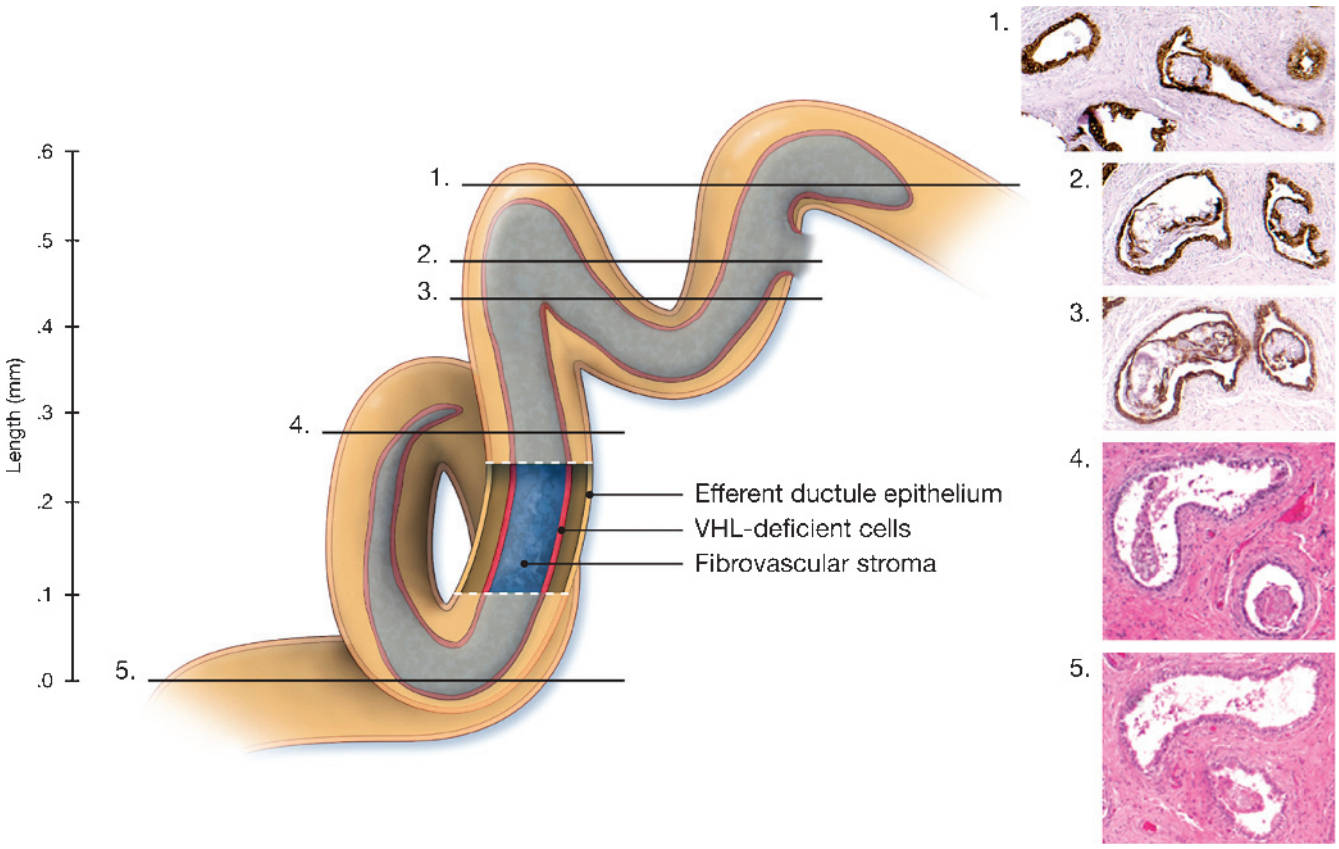

Figure 5. Neoplastic progression of intraductular papillary growth, three-dimensional reconstruction; five representative levels are shown on immunohistochemical preparations using MAK6 (1, 2, 3) or on H&E–stained sections (4, 5). Original papillary proliferation is seen in level 2. Step sections reveal the papillary proliferation to generate a tubular structure that deeply extends into the ductular system, composed of an outer rim of epithelial, VHL-deficient cells, and a central core of reactive fibrovascular tissue.

therefore be argued that up-regulation of HIF and VEGF in VHL-deficient mesonephric material may be associated with its primitive developmental state. The key event associated with developmental arrest may therefore not be the up-regulation of hypoxic stress but the failure to down-regulate it. Pathologic persistence of HIF and VEGF may therefore be associated with functional impairment of the affected cells' developmental program. Immortalization, combined with incapacity of terminal differentiation, seems to be a *condicio sine qua non* for tumorigenesis. It remains to be shown under which conditions these prerequisites are associated with cellular proliferation.

Whereas immature mesonephric material and cysts may primarily represent maldeveloped anatomic structures, papillary formation is indicative of pathologic cellular proliferation. Applying consistent concentrations of HIF1 and HIF2 antibodies, we consistently detected increased HIF2 signal compared with HIF1 signal in maldeveloped structures consistent with the recent observation of contrasting properties of HIF1 and HIF2 in VHL disease–associated renal lesions [26] (Figures 1 and 2). In areas of papillary proliferation, however, HIF1 and HIF2 signal intensities were less distinct (Figure 3), possibly indicating increased HIF1 activation to be associated with proliferative activity.

We have shown that VHL inactivation of a subset of mesonephric cells causes maldeveloped anatomic structure in epididymal tissue of VHL patients. We also demonstrated that maldevelopment can be followed by limited papillary proliferation creating a pathologic tumorlet structure. Three-dimensional reconstruction revealed a subset of papillary events to be associated with extensive neoplastic growth into the efferent ductular system, and extrapolation of this process to a later time point in time would predict a tumor with tightly intermingled neoplastic and preexistent anatomic structures (Figure 5). The distinctive intraductular extension of VHL-deficient cells is reminiscent of hamartomatous structures that have been defined as "localized, disordered differentiation during embryonic development" [27] or as tissues that have been "wrongly assembled in the course of development" [28]. At the same time, however, hamartomatous cells are defined as "nonneoplastic" [29], "mature" [30], or "adult" [31], which seems inconsistent with our identification of developmentally arrested mesonephric cells, proliferation of which constitutes epididymal neoplasia.

Whatever the accurate terminology for early VHL tumorigenesis may be, we propose it to occur in two distinct pathogenetic stages. The first stage is characterized by developmental arrest of VHL-deficient cells with subsequent structural-anatomic alterations of the epididymal tissue. The second stage is characterized by slow proliferation of a subset of VHL-deficient cells with activation/up-regulation of HIF and VEGF, associated with continuous reactive fibrovascular proliferation.

Acknowledgments

The authors are grateful to Cynthia Harris for skillful immunohistochemistry preparations; to Willie Young, Jim Rainey, and David Kleiner, Autopsy Service, Laboratory of Pathology, National Cancer

Institute; Vikki Baker and John Polite II, Histotechnology Laboratory, Laboratory of Pathology, National Cancer Institute; Ethan Tyler, Medical Illustrations, Clinical Center, National Institutes of Health, for artwork (Figure 5).

References

[1] Melmon KL and Rosen SW (1964). Lindau's disease: review of literature and study of a large kindred. *Am J Med* **36**, 595–617.

[2] Price EB Jr (1971). Papillary cystadenoma of the epididymis. A clinicopathologic analysis of 20 cases. *Arch Pathol Lab Med* **91**, 456–470.

[3] Latif F, Duh FM, Gnarra J, Tory K, Kuzmin I, Yao M, Stackhouse T, Modi W, Geil L, Schmidt L, et al. (1993). von Hippel–Lindau syndrome: cloning and identification of the plasma membrane Ca^{2+}–transporting ATPase isoform 2 gene that resides in the von Hippel–Lindau gene region. *Cancer Res* **53**, 861–867.

[4] Gläsker S, Tran MGB, Shively SB, Ikejiri B, Lonser RR, Maxwell PH, Zhuang Z, Oldfield EH, and Vortmeyer AO (2006). Epididymal cystadenomas and epithelial tumourlets: effects of VHL deficiency on the human epididymis. *J Pathol* **210**, 32–41.

[5] Vortmeyer AO, Tran M, Zeng W, Glasker S, Riley C, Tsokos M, Ikejiri B, Merrill MJ, Raffeld M, Zhuang Z, et al. (2006). Evolution of VHL tumorigenesis in nerve root tissue. *J Pathol* **210**, 374–382.

[6] Vortmeyer AO, Yuan Q, Lee YS, Zhuang Z, and Oldfield EH (2004). Developmental effects of von Hippel–Lindau gene deficiency. *Ann Neurol* **55**, 721–728.

[7] Talks KL, Turley H, Gatter KC, Maxwell PH, Pugh CW, Ratcliffe PJ, and Harris AL (2000). The expression and distribution of the hypoxia-inducible factors HIF-1alpha and HIF-2alpha in normal human tissues, cancers, and tumor-associated macrophages. *Am J Pathol* **157**, 411–421.

[8] Berkman RA, Merrill MJ, Reinhold WC, Monacci WT, Saxena A, Clark WC, Robertson JT, Ali IU, and Oldfield EH (1993). Expression of the vascular permeability factor/vascular endothelial growth factor gene in central nervous system neoplasms. *J Clin Invest* **91**, 153–159.

[9] Suchanek detection of mRNA on paraffin-embedded material of the central nervous system with DIG-labeled RNA probes. *Nonradioactive In Situ* Hybridization Application Manual, pp. 164–168. Roche Diagnostics Corporation.

[10] Burkitt HG, Young B, and Heath JW (1993). Male reproductive system. *Wheater's Functional Histology* 3rd ed., pp. 323–334. London: Churchill Livingstone.

[11] Lindau A (1926). Studien uber kleinhirnzysten. Bau, pathogenese und beziehung zur angiomatosis retinae. *Acta Path et Microbiol Scand* (Suppl 1), 1–126.

[12] Magro G, Perris R, Romeo R, Marcello M, Lopes M, Vasquez E, and Grasso S (2001). Comparative immunohistochemical analysis of the expression of cytokeratins, vimentin, and alpha-smooth muscle actin in human foetal mesonephros and metanephros. *Histochem J* **33**, 221–226.

[13] Lubensky IA, Gnarra JR, Bertheau P, Walther MM, Linehan WM, and Zhuang Z (1996). Allelic deletions of the *VHL* gene detected in multiple microscopic clear cell renal lesions in von Hippel–Lindau disease patients. *Am J Pathol* **149**, 2089–2094.

[14] Mandriota SJ, Turner KJ, Davies DR, Murray PG, Morgan NV, Sowter HM, Wykoff CC, Maher ER, Harris AL, Ratcliffe PJ, et al. (2002). HIF activation identifies early lesions in VHL kidneys: evidence for site-specific tumor suppressor function in the nephron. *Cancer Cell* **1**, 459–468.

[15] Gläsker S, Lonser RR, Tran MGB, Ikejiri B, Butman JA, Zeng W, Maxwell PH, Zhuang Z, Oldfield EH, and Vortmeyer AO (2005). Effects of VHL deficiency on endolymphatic duct and sac. *Cancer Res* **65**, 10847–10853.

[16] Richards FM, Schofield PN, Fleming S, and Maher ER (1996). Expression of the von Hippel–Lindau disease tumour suppressor gene during human embryogenesis. *Hum Mol Genet* **5**, 639–644.

[17] Pause A, Lee S, Worrell RA, Chen DY, Burgess WH, Linehan WM, and Klausner RD (1997). The von Hippel–Lindau tumor-suppressor gene product forms a stable complex with human CUL-2, a member of the Cdc53 family of proteins. *Proc Natl Acad Sci USA* **94**, 2156–2161.

[18] Lonergan KM, Iliopoulos O, Ohh M, Kamura T, Conaway RC, Conaway JW, and Kaelin WG Jr (1998). Regulation of hypoxia-inducible mRNAs by the von Hippel–Lindau tumor suppressor protein requires binding to complexes containing elongins B/C and Cul2. *Mol Cell Biol* **18**, 732–741.

[19] Lisztwan J, Imbert G, Wirbelauer C, Gstaiger M, and Krek W (1999). The von Hippel–Lindau tumor suppressor protein is a component of an E3 ubiquitin–protein ligase activity. *Genes Dev* **13**, 1822–1833.

[20] Maxwell PH, Wiesener MS, Chang GW, Clifford SC, Vaux EC, Cockman ME, Wykoff CC, Pugh CW, Maher ER, and Ratcliffe PJ (1999). The tumour suppressor protein VHL targets hypoxia-inducible factors for oxygen-dependent proteolysis. *Nature* **399**, 271–275.

[21] Cockman ME, Masson N, Mole DR, Jaakkola P, Chang GW, Clifford SC, Maher ER, Pugh CW, Ratcliffe PJ, and Maxwell PH (2000). Hypoxia inducible factor-alpha binding and ubiquitylation by the von Hippel–Lindau tumor suppressor protein. *J Biol Chem* **275**, 25733–25741.

[22] Ohh M, Park CW, Ivan M, Hoffman MA, Kim TY, Huang LE, Pavletich N, Chau V, and Kaelin WG (2000). Ubiquitination of hypoxia-inducible factor requires direct binding to the beta-domain of the von Hippel–Lindau protein. *Nat Cell Biol* **2**, 423–427.

[23] Iliopoulos O, Levy AP, Jiang C, Kaelin WG Jr, and Goldberg MA (1996). Negative regulation of hypoxia-inducible genes by the von Hippel–Lindau protein. *Proc Natl Acad Sci USA* **93**, 10595–10599.

[24] Krieg M, Haas R, Brauch H, Acker T, Flamme I, and Plate KH (2000). Up-regulation of hypoxia-inducible factors HIF-1alpha and HIF-2alpha under normoxic conditions in renal carcinoma cells by von Hippel–Lindau tumor suppressor gene loss of function. *Oncogene* **19**, 5435–5443.

[25] Nanka O, Valasek P, Dvorakova M, and Grim M (2006). Experimental hypoxia and embryonic angiogenesis. *Dev Dyn* **235**, 723–733.

[26] Raval RR, Lau KW, Tran MG, Sowter HM, Mandriota SJ, Li JL, Pugh CW, Maxwell PH, Harris AL, and Ratcliffe PJ (2005). Contrasting properties of hypoxia-inducible factor 1 (HIF-1) and HIF-2 in von Hippel–Lindau–associated renal cell carcinoma. *Mol Cell Biol* **25**, 5675–5686.

[27] Rubin E and Farber JL (1999). *Pathology.* 3rd ed. Philadelphia, PA: Lippincott Raven.

[28] Majno G and Joris I (2004). *Cells, Tissue, and Disease: Principles of General Pathology.* 2nd ed. New York, NY: Oxford University Press.

[29] Stevens A and Lowe JS (2000). *Pathology: Illustrated Review in Color.* 2nd ed. St. Louis, MO: Mosby.

[30] Kumar V, Abbas AK, and Fausto N (2005). *Robbins and Cotran. Pathologic Basis of Disease.* Philadelphia, PA: Elsevier Saunders.

[31] Chandrasoma P and Taylor CR (1998). *Concise Pathology.* 3rd ed. Norwalk, CT: Appleton & Lange.